fluids

MDPI

Article

Flow Dynamics in a Model of a Left Ventricle with Different Mitral Valve Orientations

Ghassan Maraouch * and Lyes Kadem

Laboratory of Cardiovascular Fluid Dynamics, Concordia University, Montréal, QC H3G 1M8, Canada; kadem@encs.concordia.ca

* Correspondence: g_maraou@encs.concordia.ca

Abstract: The formation of vortex rings at valve leaflets during ventricular inflow has been a topic of interest for many years. It is generally accepted nowadays that the purpose of vortex rings is to conserve energy, reduce the workload on the heart, and minimize particle residence time. We investigated these claims by testing three different levels of annulus angle for the mitral valve: a healthy case, a slightly angled case (20°), and a highly angled case (46°). Circulation was determined to be reversed in the non-healthy case, with a dominant counterclockwise rotation instead of clockwise. Viscous energy dissipation was highest in the slightly angled case, followed by the healthy case and then the highly angled case. A Lagrangian analysis demonstrated that the healthy case resulted in the least amount of stasis, requiring eight cardiac cycles to evacuate 99% of initial ventricle volume compared to the 16 and 13 cardiac cycles required by the slightly angled and highly angled cases, respectively.

Keywords: mitral valve; left ventricular flow; cardiac flow; transmitral flow; mitral valve replacement; vortex rings

Citation: Maraouch, G.; Kadem, L. Flow Dynamics in a Model of a Left Ventricle with Different Mitral Valve Orientations. *Fluids* **2021**, *6*, 428. https://doi.org/10.3390/fluids6120428

Academic Editor: Dimitrios Mathioulakis

Received: 30 September 2021
Accepted: 16 November 2021
Published: 26 November 2021

1. Introduction

The heart is the organ with the crucial role of pumping blood throughout our body, allowing our cells to properly perform their functions, making life possible. From a practical point of view, the heart is quite impressive, given its ability to accommodate different levels of activities requiring increased blood flow. One of the key components of the heart is the left ventricle. During the filling phase of the ventricle (diastole), the chamber begins filling with freshly oxygenated blood. The filling phase is characterized by an asymmetric jet that smoothly propagates towards the outflow tract [1,2]. The jet is not continuous; rather, it is characterized by two phases—the E wave (ventricular dilation) and the A wave (atrial contraction) [3–5]. The formation of a vortex ring surrounding the central jet is due to the boundary layer separation from the mitral valve leaflet, and the observed asymmetry in the ring sizes occurs because of the asymmetric nature of the mitral valve leaflets. It is now generally accepted that the purpose of this mechanism of fluid transport is to minimize the amount of energy dissipation, reduce the workload on the ventricle, and minimize the residence time of blood in the ventricle [1].

Multiple pathologies have been identified to affect the dynamics in the left ventricle. For instance, aortic regurgitation causes a regurgitant jet to form in the ventricle from the aortic valve (AV) [6]. This regurgitant jet collides with the inflow jet, altering the flow dynamics [6]. Dilated cardiomyopathy is characterized by an enlarged chamber, which results in a more spherical jet that is not fully dissipated nor ejected during systole [7,8]. Replacing the mitral valve (MV), whether with a mechanical or bioprosthetic valve, has also been identified as a primary cause for an alteration in the mitral flow [9,10]. Bileaflet mechanical valves will result in different flow patterns depending on their orientation; for instance, placing the valve in an anatomical position will conserve the vortex flow pattern direction, whereas the anti-anatomical position will result in a reversal in the direction [10]. Additionally, the bileaflet mechanical valves generate side jets [7]. Of particular interest,

bioprosthetic valves have been shown to cause a reversal in the flow rotation, even in cases where the annulus angle is within the range of the annulus angle for patients that underwent valve repair [9]. In fact, due to the symmetry of the trileaflet bioprosthetic valve, the asymmetry of the jet is lost, which causes the flow path to deviate from its normal path [11]. This deviation has been observed to result in a cross-flow pattern with a rotation in the reversed direction at the apex [11]. As a consequence, an increase in energy loss occurs because of the collision of the inflow jet with the anteroseptal wall during the filling phase and the mitral valve during the ejection phase [9].

With these findings in mind, using an in vitro model, we investigated the effects that three mitral valve annulus angles have on the flow dynamics. Quantification of the viscous energy dissipation, the circulation, and the particle residence time was of particular interest considering the findings previously mentioned.

2. Methodology

The effect of different orientations of the mitral valve was investigated using a custom-made in vitro heart simulator (see Figure 1 for a schematic of the heart simulator). Transparent silicone (Silastic T4) was the material of choice for manufacturing of the left ventricle, aorta, and left atrium due to its desirable mechanical property and extensive use in similar research [6,12–15]. Modeling of the left ventricle for this study was symmetrically shaped with an angle of 28° between the inflow and outflow tract (see Figure 2) and with geometric properties as described in [3]. Changing the mitral valve orientation was achieved by sowing the valve to a 3D printed part with different angles. We tested a total of three different valve orientations, the first case being our control (i.e., properly positioned position). An angle of 20° for the smallest misoriented angle was used, measured from the center of the jet using the line that joins the center of the mitral valve with the apex as a reference axis (see Figure 3). For the most severe case, an angle of 46° was used.

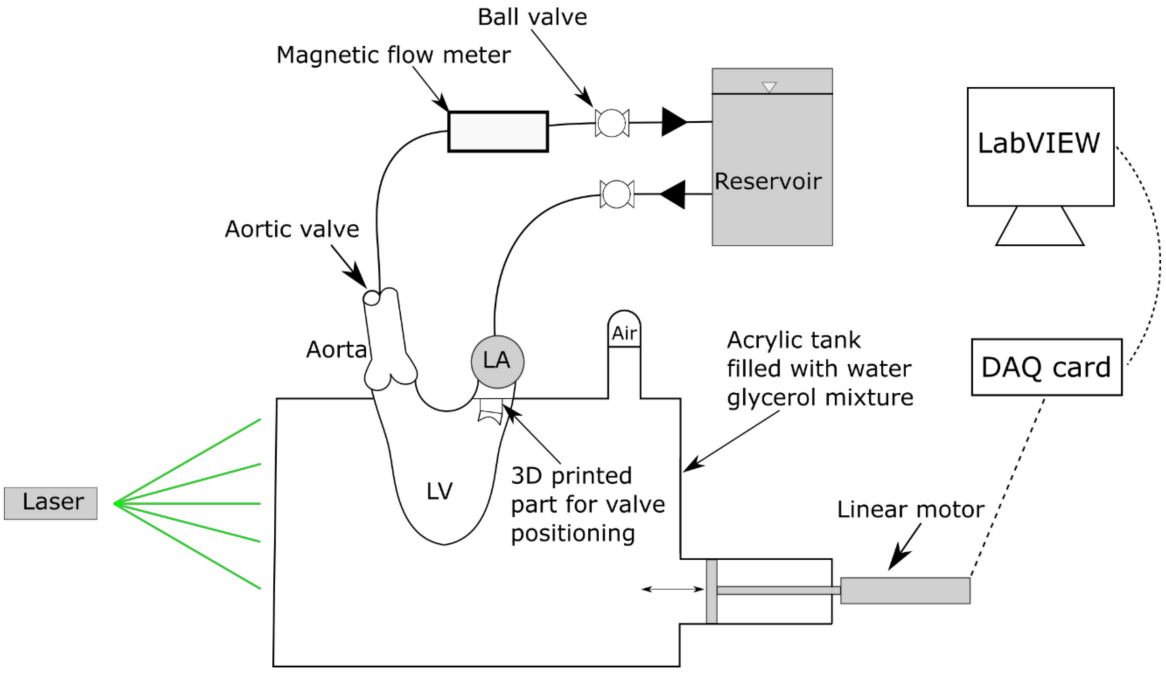

Figure 1. Schematic of the heart simulator used. Ball valves are used to regulate the pressure and flow rate throughout the system. Actuation of the system is done hydraulically via the linear motor. The camera is placed out of the page, orthogonal to the laser sheet, with the recording window being into the page.

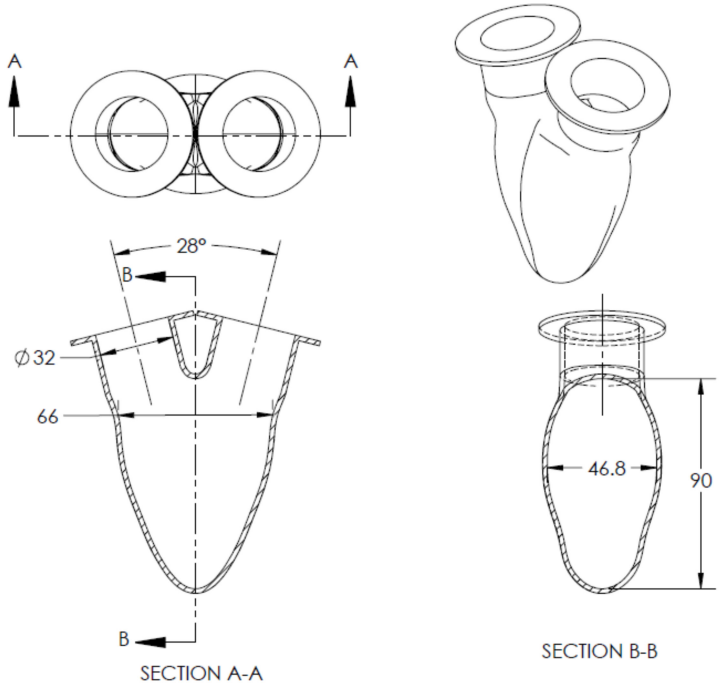

Figure 2. Internal dimensions of the left ventricle used in the simulator. The thickness and outer dimensions will vary depending on the number of layers of silicone applied.

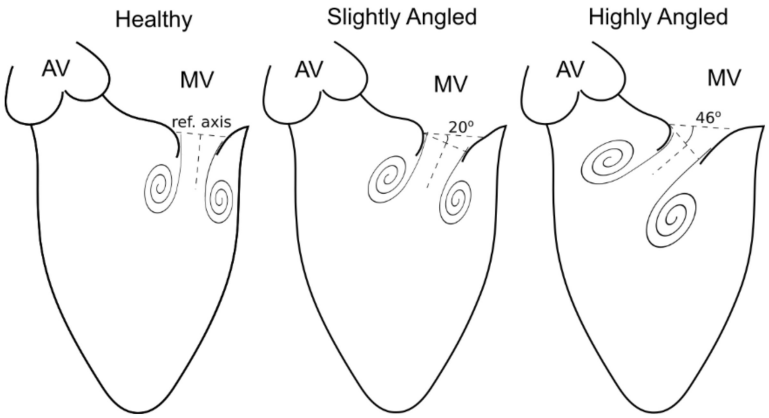

Figure 3. Mitral inflow for the healthy, slightly angled, and highly angled cases. The healthy inflow corresponds to a jet that is aligned with the apex such that the clockwise vortex swirls around the apex. The least severe case is oriented at an angle of 20°, using the orientation of the healthy case as a reference axis. The most severe case is tilted at an angle of 46°.

The working fluid to mimic blood was a mixture of water–glycerol with a volumetric ratio of 60:40, giving it a refractive index of n = 1.39, density of ρ = 1100 kg/m^3, and dynamic viscosity of μ = 4.2 cP at a temperature $T \approx 23.0$ °C. A biological tricuspid valve of a 25 mm diameter was used for both the aortic and mitral valves.

Actuation of the heart simulator was performed using a magnetic linear motor (PS01-37 × 120) controllable through LabVIEW (National Instruments, Austin, TX, USA) with variable heart rate, stroke length, and position waveform (see Figure 4). Use of the motor was to hydraulically contract and relax the left ventricle, located inside an acrylic tank filled with the water–glycerol mixture, which generated a flow profile depending on the waveform used. Duration of systole and diastole was set according to the equations in [16]. The A wave was integrated into the motor waveform, which is more physiologically correct, compared to having a direct contraction at the left atrium. Filling the tank with the working

fluid was performed to prevent image distortion from the change of refraction index. A small air gap, closed to atmosphere, was kept in the tank to adjust the left ventricle compliance.

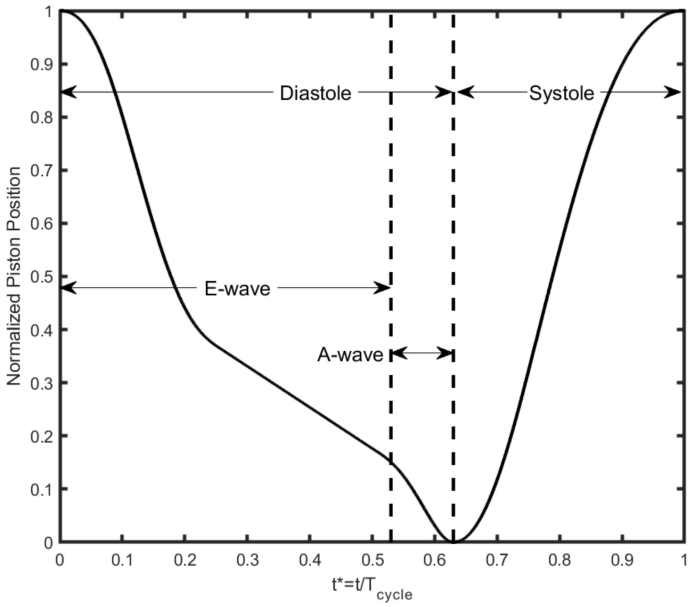

Figure 4. Position waveform used to actuate the linear motor in the heart simulator. The position and time are normalized so that different stroke lengths and heart rates can be selected. The A wave is integrated in the waveform.

Calibration of the system was achieved by tuning ball valves, which affects the flowrate and pressure (see Figure 1). The first ball valve is located upstream from the left atrium, whereas the second valve is downstream from the aorta. Instantaneous pressure was measured using a fiber-optic sensor (FISO FOP-M260, Québec, QC, Canada with FISO FPI HR-2 module, sampling rate of 125 Hz, working range of −300 mmHg to 300 mmHg with an accuracy of ± 3 mmHg). Recording of the pressure and any other measurement followed after about 20 cardiac cycles to allow the system to stabilize. The average flow rate was measured by a magnetic inflow flow meter (ProSense® FMM75-1002, München, Germany, accuracy ±0.31 L/min, resolution of 0.076 L/min). A summary of all the experimental parameters can be found under Table 1.

Table 1. Summary of experimental conditions.

Working Fluid Conditions		**Simulator Conditions**	
Water–glycerol ratio	60:40	Heart rate	80 bpm
Density (ρ)	1100 kg/m^3	Cardiac cycle period	0.75 s
Dynamic viscosity (μ)	0.0042 Pa·s	Systole duration	0.28 s
		Mitral valve diameter	25 mm
		Aortic valve diameter	25 mm
		Cardiac output	3.1 ± 0.31 L/min
		Mitral inflow Womersley number (Wo) [a]	18.52
		Mitral inflow mean Reynolds number (Re) [a]	689.17

[a] The nominal diameter of the mitral valve is used for the calculations of the Womersley and Reynolds number.

Particle image velocimetry (PIV) was the method of choice for measuring the vector field following the guidelines in [17,18]. Tracer particles made of polyamide with a diameter of 50 ± 20 μm were used for measurements. A LDY301 Nd:YLF dual-pulsed laser (Litron Lasers Ltd., Rugby, England) with a wavelength of 527 nm was used to illuminate the tracers. Image capture was performed using a Phantom V9.1 (Vision Research, Inc., Wayne, NJ, USA) high-speed camera with a recording frequency of 600 Hz for the healthy and slightly angled cases and 450 Hz for the highly angled case. The field of vision was

readjusted whenever the angle of the mitral valve was repositioned so that the image could be calibrated. Post-processing of the PIV recordings was performed using Davis 7.2 (LaVISION GmbH, Göttingen, Germany). A multi-pass algorithm was used for post-processing; the first pass utilizes a 64 × 64 interrogation window, followed by a 32 × 32 interrogation window, and then three passes were made using a 16 × 16 window. This resulted in a spatial resolution of approximately 0.55 mm. Filtering of the spurious vectors outside the boundaries was performed by using an in-house edge-detection software, which recognizes the boundaries of the ventricle. The velocity field measurements have an uncertainty less than 5%. Recording of each case was repeated at least three times.

3. Results and Discussion

3.1. Effects of Misalignment

One of the most notable observations in altering the natural orientation of the mitral valve is the change in the trajectory of the transmitral jet (Figure 5). In the healthy case (i.e., properly positioned, see Video S1 "Healthy" in Supplementary Materials), we note that the jet propagates towards the apex along the lateral wall. Due to the wall interaction, the counterclockwise (CCW) vortex ring dissipates rapidly, leaving the clockwise (CW) vortex ring to dominate in the flow. This dissipation of the CCW ring results in an optimized flow because of the smooth redirection of the jet along the apex into the outflow tract, supposedly to minimize the amount of energy loss and to minimize stasis. Adding a slight tilt to the mitral valve (see Video S2 "Slightly Angled" in Supplementary Materials) results in a jet that propagates away from the lateral wall; this new trajectory causes the CCW vortex ring to remain in existence throughout its propagation. Eventually, the jet will hit the interventricular septum, causing the two vortex rings to separate from the central jet. This causes the ventricle to encapsulate a new recirculation region. There now exist two regions, each region having a dominant rotation in the direction of a vortex ring. This altered trajectory was also noted in Kheradvar et al. [7] and Pedrizzetti et al. [11]. Increasing the severity of the tilt (see Video S3 "Highly Angled" in Supplementary Materials) causes the jet to hit the interventricular septum, but this time closer to the outflow tract. This altered trajectory also results in a recirculation region.

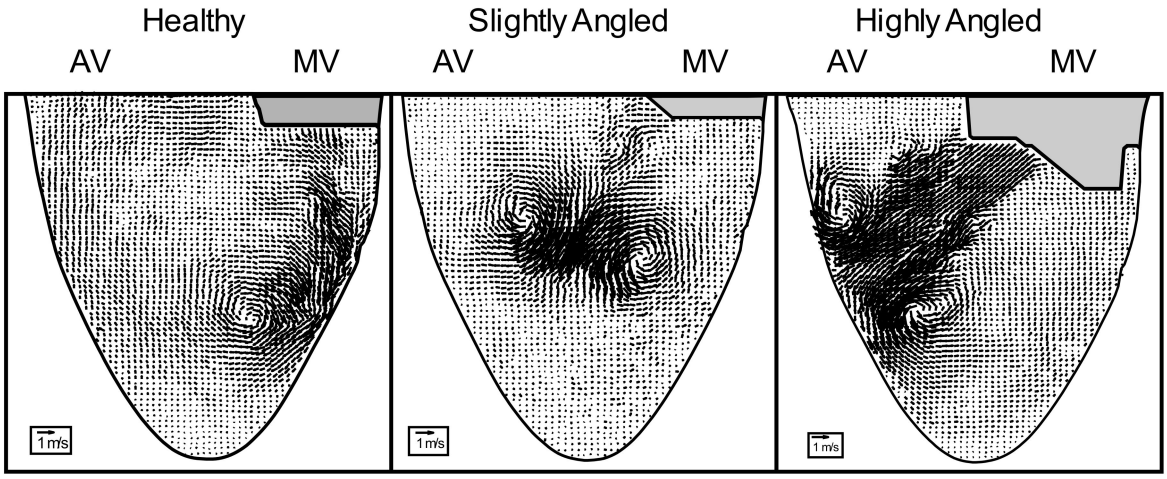

Figure 5. Vector field portraying the different inlet jet for the different orientation of the mitral valve. The corresponding time of the cycle at which this occurs is $t^* = 0.5$.

3.2. Circulation

Figure 6 displays the temporal evolution of the circulation. A properly positioned mitral valve results in a dominant clockwise circulation, which is illustrated by the negative sign of the circulation. The dominance of this clockwise direction in this particular flow is because of the dissipation that occurs from the wall interactions with the CCW vortex ring, leaving only the CW vortex ring to contribute to the rotation of the flow. In contrast,

when the mitral valve is tilted, the circulation is no longer negative. Instead, the flow has a dominant counterclockwise direction, characterized by the positive sign of the circulation.

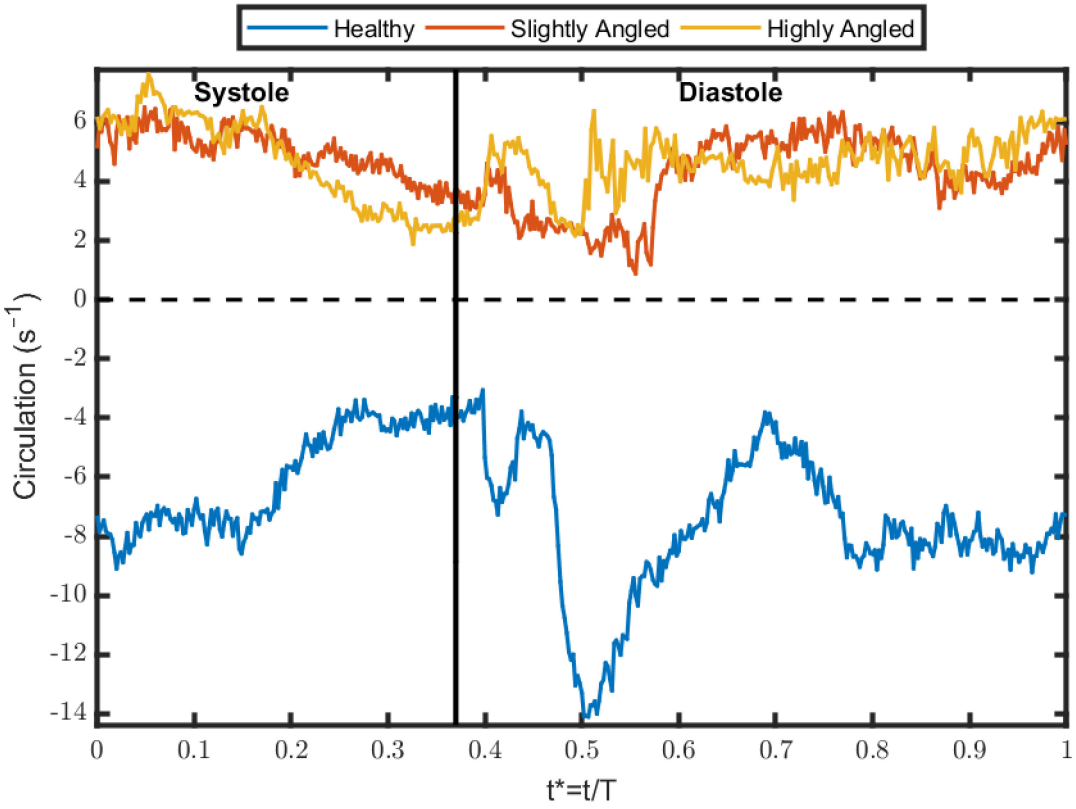

Figure 6. Circulation per unit area (s^{-1}) of the flow. Adding a tilt to the mitral valve results in the flow to have a dominant counterclockwise direction. The vertical line separates the time period between systole and diastole.

This phenomenon is caused by the lack of dissipation of the CCW vortex ring from the wall interactions. Incidentally, once the jet collides with the interventricular septum, the two vortex rings separate from the central jet. The CCW vortex ring propagates into the more open apical area, resulting in the recirculation area previously described. In the case of the CW vortex, it is now subject to interactions with the wall of the interventricular septum as it propagates towards the outflow tract, resulting in a reduction of its strength. This ultimately causes the flow to have a dominant CCW direction. The highly angled case also results in the circulation reversing in direction. Interestingly, increasing the severity of the valve tilt seems to have little effect on the strength of the circulation. We verify this observation by computing the mean circulation throughout the entire cardiac cycle, as seen in Figure 7. The average circulation in the properly positioned valve has a higher magnitude than the two other cases in the averaging period ($p << 0.05$). On the other hand, the slightly angled and the highly angled cases both have similar magnitudes ($p = 0.12$). This observation would suggest that slightly tilting the valve would cause the circulation to reverse in direction but increasing its severity would not lead to a significant increase in the magnitude.

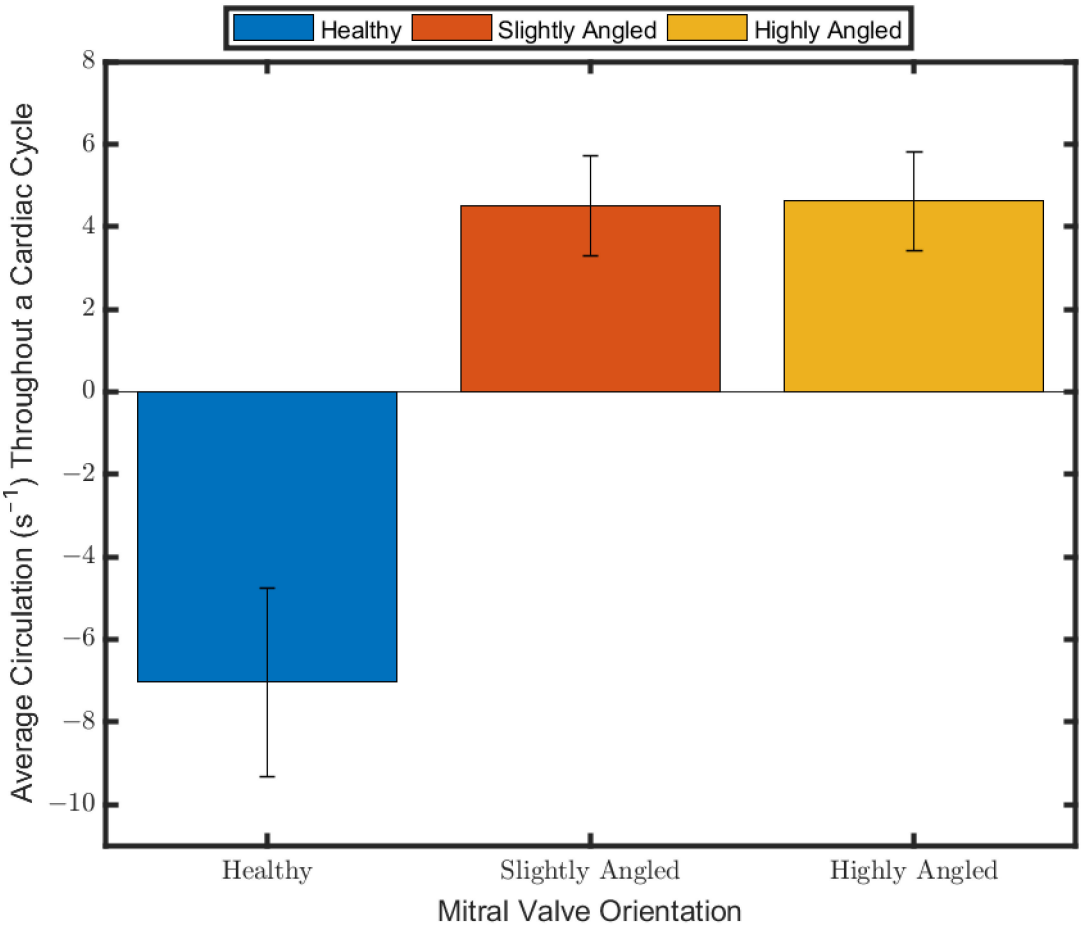

Figure 7. Temporal average circulation per unit area of the flow over the entire cardiac cycle. The *p*-values between the healthy case and slightly angled case, between the healthy case and highly angled case, and between the slightly angled and highly angled case are $p < 0.01$, $p < 0.01$, and $p = 0.12$, respectively. Note that the absolute value of the circulation was used.

Reversal of the vortex direction has been previously observed by Pedrizzetti et al. [11], Akiyama et al. [9], and Nakashima et al. [10]. Faludi et al. [19] also observed this reversal and quantified the relative pulsatile vorticity strength (RS) and vortex relative pulsatile vorticity strength (VRS) (refer to Reference [19] for definitions). Ultimately, their results indicate that the VRS itself is not statistically different following the implantation of a bioprosthetic valve compared to the healthy case, but there was a statistical difference in the RS value, which they attribute to higher energy loss in the flow. However, their metric focuses more on the pulsatility aspect of the vortices rather than the strength.

3.3. Viscous Energy Dissipation

Viscous energy dissipation (VED) is a metric that has been extensively used to characterize the energy loss due to the viscous effects in the flow [4,6,9,20]. This quantity can be described as one that quantifies the efficiency of the flow to preserve kinetic energy. Pedrizzetti et al. [11] have noted that viscous energy dissipation is minimized in an optimally positioned mitral valve. Surprisingly, our results do not lead to the same straightforward conclusion (see Figure 8). Throughout systole, the healthy case has a lower VED than the slightly angled case until a certain time instance ($t^* \approx 0.1$), at which point the healthy case becomes more dissipative than the latter. The highly angled case is less dissipative throughout systole compared to the two other cases. Following the beginning of the filling phase, the VED increases as the mitral valve opens and the transmitral jet begins propagating. In the healthy case, the VED increases rapidly, peaks shortly after the beginning of the filling phase, and then remains relatively steady before experiencing a

drop. The VED then steadily increases until a second peak and then gradually decreases until the end of the cycle. In the slightly angled case, the VED increases more steadily until a peak is reached, followed by a gradual decline until the end of the cycle. Similarly, the highly angled case portrays a similar pattern, except that the peak of the VED is higher and is reached sooner. Additionally, the decrease in the VED following the peak is more drastic.

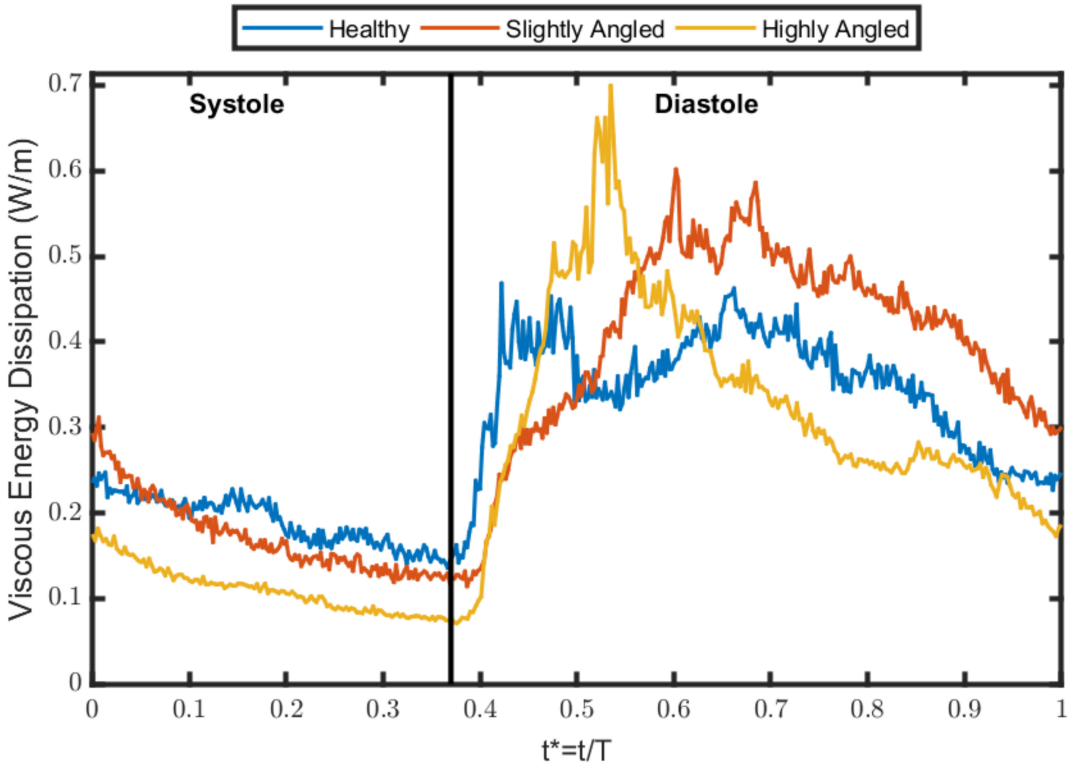

Figure 8. Temporal evolution of viscous energy dissipation (W/m) per cardiac cycle. Note that the vertical line separates the ejection phase (left) and filling phase (right).

We summarized the VED by computing the temporal average values (Figure 9) for the entire cycle. The highly angled case appears to be the least dissipative, followed by the healthy case and then the slightly angled case when averaging throughout the cardiac cycle and diastole ($p < 0.05$ between each case). Hence, our evidence suggests that simply altering the trajectory will not necessarily increase the viscous energy dissipation. The in vivo study of Akiyama et al. [9] quantified the energy loss change in patients pre- and post-valve replacement and repair surgery. Their results indicate that the valve replacement, which leads to the altered flow trajectory, would result in more energy loss compared to the repair group, which maintains the physiological flow for most cases. A more relatable study are the findings of Watanabe et al. [21], who have shown that for a severe deviation in the flow trajectory, the increased workload of the heart is not undoubtedly higher in the non-physiological flow. This was the case in their 100 bpm case, but not for the 60 bpm case. Regardless, they argued that the workload difference was negligible, and that the formation of vortex rings serves as a primary mechanism to minimize particle residence time. Seo et al. [22] also suggested that the energy dissipation in the flow is negligible compared to the workload of the ventricle.

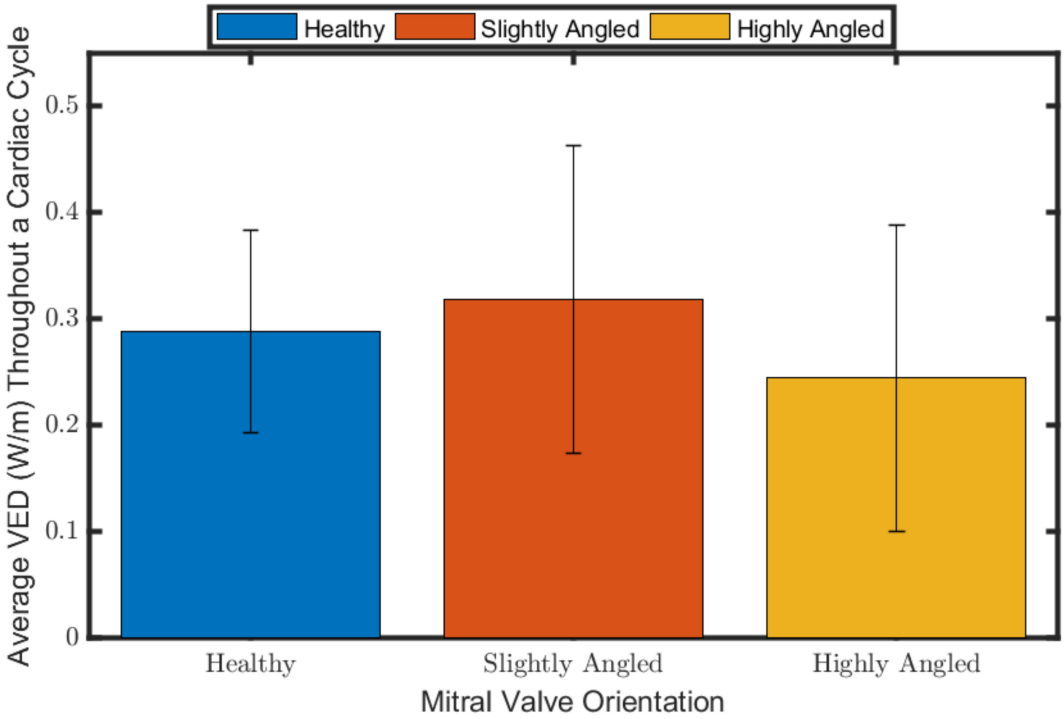

Figure 9. Average viscous energy dissipation (W/m) throughout a cardiac cycle, systole, and diastole. The p-values between the healthy case and slightly angled case, between the healthy case and highly angled case, and between the slightly angled and highly angled case are $p < 0.01$, $p < 0.01$, and $p < 0.01$, respectively.

3.4. Ventricular Washout

Residence time is another underlying consequence in altered flow patterns that has led to various research on it and different techniques to quantify it [23–28]. The importance of minimizing the residence time of blood in the ventricle is to reduce the formation of clots due to flow stagnation [29,30], which can lead to stroke. We investigated blood stasis by using a metric known as ventricular washout (Figure 10), which was described by Seo et al. [22]. This metric quantifies how many cycles are required to eject 99% of the initial blood volume. Ventricular washout is computed as:

$$k_{1\%} = \frac{\log(0.01)}{\log(RR)}$$

The parameter RR is known as the residual volume ratio, which is the ratio of the residual ventricular volume after a cardiac beat over the total initial ventricular volume prior to the ejection. Our results seem to favor the normal flow pattern in terms of minimizing stasis, with a ventricular washout requiring approximately 7.25 cycles. The slightly angled case promotes more stasis than the highly angled case, each requiring 16 and 13 cycles, respectively, meaning that the most severe case is not necessarily the least optimal for particle stasis. Seo et al. [22] noted that the ventricular washout was also higher in their case with an altered trajectory (synonymous with our slightly angled case); however, it is also worth mentioning that their testing conditions were not similar to their healthy case.

Pathlines using virtual particles for each case are plotted to better understand why one case might be superior to one another for particle ejection. As seen in Figure 11, the healthy case, which minimizes stasis, has a tendency to push particles towards the outflow tract. In contrast, the flow generated in the slightly angled case and in the highly angled case tends to trap the particles in the ventricle for longer periods close to the apex.

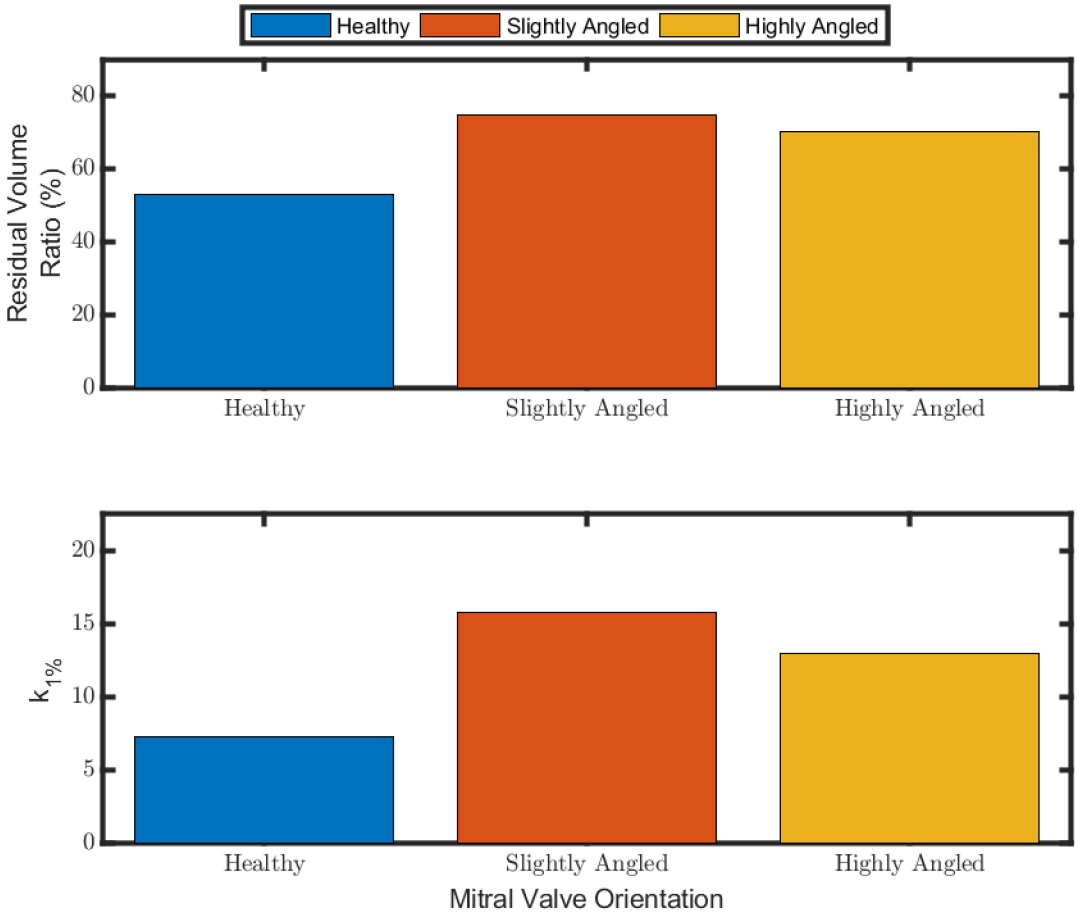

Figure 10. Residual volume ratio and the ventricular washout ($k_{1\%}$).

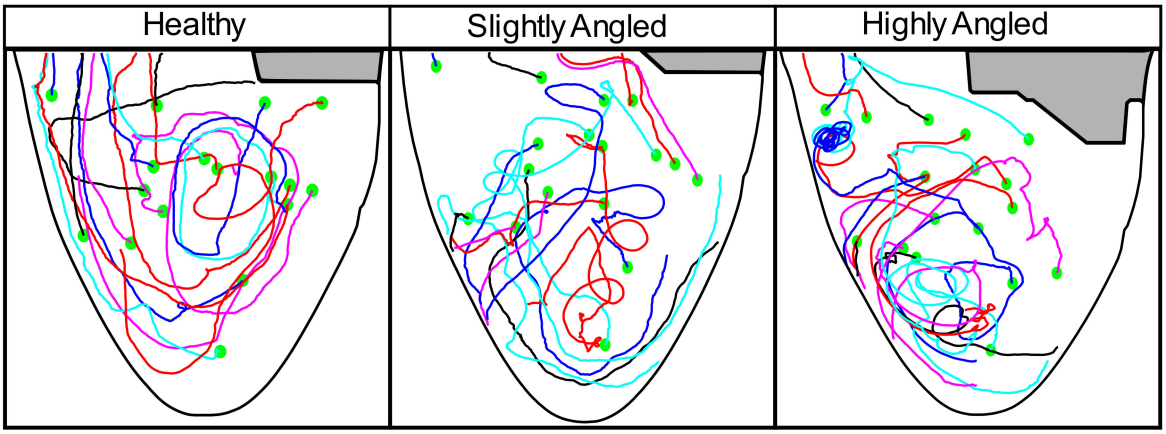

Figure 11. Pathlines over a cardiac cycle for some virtual particles. The green dot represents the initial position. Particles that leave the domain are considered ejected and are no longer tracked.

3.5. Discussion

The flow patterns that we observed seem to be in line with those observed in the literature. Pedrizzetti et al. [11] noted, with a bileaflet mechanical prosthetic heart valve, that there is a crossed flow pattern appearing in the left ventricle. They simulated this flow by adding a slight tilt to the mitral inflow in their numerical solver, which resulted in an inlet jet that hit the interventricular septum at a location similar to our slightly angled case. The numerical study by Watanabe et al. [21] also observed a similar flow pattern; their mitral valve was angled at a more severe angle, similar to our highly angled case.

Similar observations were also noted in clinical studies. Nakashima et al. [10] distinguished two overall flow directions: clockwise and counterclockwise. The counterclockwise flow occurred with a mechanical heart valve placed in the anti-anatomical position and with a bioprosthetic valve. Akiyama et al. [9] instead described the flow as normal (physiological flow) or abnormal (crossed flow pattern).

While the previous references all noted the altered flow dynamics, there is a lack in the quantification of this observation. The computation of circulation addresses this. Indeed, what the circulation has revealed is that there is an overall counterclockwise flow in a physiological flow when taken from our field of view. By altering the annulus angle of the mitral valve, the circulation reverses in direction, resulting in an overall clockwise direction; this was observed in the slightly angled and highly angled case. This agrees with the observations noted in the literature. Interestingly, the circulation between the two misaligned cases is not statistically different.

The analysis of viscous energy dissipation showed some discrepancies with the literature. It is well accepted that the vortex ring in the mitral inflow aids in minimizing the energy dissipation in the flow, reducing the workload of the heart. This idea was supported by Pedrizzetti and Domenichini [4], which demonstrated that the flow patterns in a physiological flow are optimized to reduce energy dissipation. However, their study was criticized by Seo and Mittal [22], who argued that their study is not conclusive for an adult heart because the study of Pedrizzetti and Domenichini [4] modeled an infant's heart, which has a lower Reynolds number. Later on, Pedrizzetti et al. [11] performed a numerical simulation study by adding a slight tilt to the mitral valve after observing a crossed flow pattern in patients with mechanical heart valves. Their study led to the conclusion that, indeed, the physiological flow reduces the amount of energy loss compared to the altered flow. We obtained a similar conclusion when comparing the healthy case and slightly angled case, that is, the slightly angled case is more dissipative than the healthy case. Seo and Mittal [22] also performed a numerical simulation study and their results led to a different conclusion. They studied four different flows: three of them had a normal flow pattern but with different inputs (i.e., E/A ratio and Reynolds number). The fourth case (which they denoted as Case D) had a crossed flow pattern and was less dissipative than their case C, which had a normal flow and similar inputs. However, they argued that the difference in viscous energy dissipation was negligible when considering the total work required by the ventricle.

Our conclusion becomes different once we consider the highly angled case, which was determined to be the least dissipative. The study we found to be most synonymous with this angle severity is that by Watanabe et al. [21]. They did not compute viscous energy dissipation; rather, they looked at the external work required by the ventricle. Their results showed the physiological flow required less work than the non-physiological flow at 60 bpm, but the opposite was true at 100 bpm. The clinical study of Akiyama et al. [9] investigated energy loss change (ELC), which they defined as the ratio of average energy dissipation post-procedure and pre-procedure. More specifically, they studied the ELC in patients that had either valve repair or valve replacement. Overall, their results indicate that the ELC is lower in the repair group because the vortex pattern remained normal, whereas the replacement group tended to have an abnormal vortex pattern. However, it is worth noting that they also had some instances in the replacement group that had an ELC lower than 100, despite having an abnormal vortex pattern, which would indicate that the energy loss is lower post-procedure, but it is important to consider the condition of the patient pre-procedure. Our results highly suggest that evaluating the performance of the left ventricle based on a single parameter, viscous energy dissipation, might not be optimal. Multiple parameters have to be used, including viscous energy dissipation, the residual volume ratio, and the ventricular washout ($k_{1\%}$).

Ventricular washout is the next quantity that was analyzed. Seo and Mittal [22] performed a similar analysis, for which they determined the case with the altered mitral valve angle to have the longest $k_{1\%}$. Watanabe et al. [21] also performed an analysis on

stasis, and their conclusion is similar: increasing the mitral valve angle will require more cardiac cycles to eject old blood. Both these studies agree with our results: both our slightly angled and highly angled led to more stasis than the healthy case. However, we determined the highly angled case to also lead to less stasis than the slightly angled case.

Essentially, what we determined is that properly aligning the mitral valve is important because to do otherwise would promote stasis in the left ventricular. This is especially important with the rise in popularity in transcatheter mitral valve replacement, which can result in the mitral valve not being properly oriented.

4. Limitations of the Study

This study analyzed the flow from a two-dimensional perspective. It goes without saying that the flow is three-dimensional, and further analysis is required to obtain a more precise picture of the flow. Nevertheless, this study was still insightful given the extensive use of 2D in vivo using echo imaging.

5. Conclusions

We investigated three different orientations for the mitral valve. It was determined that the physiological flow generates a dominant clockwise rotation in the ventricle. Altering the orientation of the valve results in a reversal in the rotation direction, giving it a dominant counterclockwise rotation. This was observed in the two misaligned cases. The viscous energy dissipation was then investigated, which has shown that the physiological flow is not necessarily the best for minimizing energy dissipation. A Lagrangian analysis was then performed to investigate the ventricular washout, which has demonstrated to be a metric that favors in healthy case because of the lower number of cycles required to clear out old blood, although the highly angled case was also observed to be better than the slightly angled case in this metric. Overall, our results seem to indicate that maintaining the physiological flow is more favorable for reducing stasis rather than minimizing energy dissipation.

Supplementary Materials: The following are available online at https://www.mdpi.com/article/10.3390/fluids6120428/s1, Video S1: Healthy; Video S2: Slightly Angled; Video S3: Highly Angled.

Author Contributions: Conceptualization, G.M. and L.K.; investigation, G.M.; writing—original draft preparation, G.M.; supervision, L.K. All authors have read and agreed to the published version of the manuscript.

Funding: This work is supported by a grant from the Natural Sciences and Engineering Research Council of Canada (Grant No. 343164-07).

Institutional Review Board Statement: Not applicable.

Informed Consent Statement: Not applicable.

Data Availability Statement: Not applicable.

Conflicts of Interest: The authors declare no conflict of interest.

References

1. Kilner, P.J.; Yang, G.-Z.; Wilkes, A.J.; Mohiaddin, R.H.; Firmin, D.; Yacoub, M.H. Asymmetric redirection of flow through the heart. *Nature* **2000**, *404*, 759–761. [CrossRef]
2. Bellhouse, B.J. Fluid mechanics of a model mitral valve and left ventricle. *Cardiovasc. Res.* **1972**, *6*, 199–210. [CrossRef]
3. Di Labbio, G.; Vétel, J.; Kadem, L. Material transport in the left ventricle with aortic valve regurgitation. *Phys. Rev. Fluids* **2018**, *3*, 113101. [CrossRef]
4. Pedrizzetti, G.; Domenichini, F. Nature Optimizes the Swirling Flow in the Human Left Ventricle. *Phys. Rev. Lett.* **2005**, *95*, 108101. [CrossRef]
5. Wang, J.; Gao, Q.; Wei, R.; Wang, J. Experimental study on the effect of an artificial cardiac valve on the left ventricular flow. *Exp. Fluids* **2017**, *58*, 1–17. [CrossRef]
6. Di Labbio, G.; Kadem, L. Jet collisions and vortex reversal in the human left ventricle. *J. Biomech.* **2018**, *78*, 155–160. [CrossRef] [PubMed]

7. Kheradvar, A.; Houle, H.; Pedrizzetti, G.; Tonti, G.; Belcik, T.; Ashraf, M.; Lindner, J.R.; Gharib, M.; Sahn, D. Echocardiographic Particle Image Velocimetry: A Novel Technique for Quantification of Left Ventricular Blood Vorticity Pattern. *J. Am. Soc. Echocardiogr.* **2010**, *23*, 86–94. [CrossRef] [PubMed]
8. Kim, I.C.; Hong, G.R. Intraventricular Flow: More than Pretty Pictures. *Heart Fail. Clin.* **2019**, *15*, 257–265. [CrossRef] [PubMed]
9. Akiyama, K.; Nakamura, N.; Itatani, K.; Naito, Y.; Kinoshita, M.; Shimizu, M.; Hamaoka, S.; Kato, H.; Yasumoto, H.; Nakajima, Y.; et al. Flow-dynamics assessment of mitral-valve surgery by intraoperative vector flow mapping. *Interact. Cardiovasc. Thorac. Surg.* **2017**, *24*, 869–875. [CrossRef] [PubMed]
10. Nakashima, K.; Itatani, K.; Kitamura, T.; Oka, N.; Horai, T.; Miyazaki, S.; Nie, M.; Miyaji, K. Energy dynamics of the intraventricular vortex after mitral valve surgery. *Heart Vessel.* **2017**, *32*, 1123–1129. [CrossRef]
11. Pedrizzetti, G.; Domenichini, F.; Tonti, G. On the Left Ventricular Vortex Reversal after Mitral Valve Replacement. *Ann. Biomed. Eng.* **2010**, *38*, 769–773. [CrossRef]
12. Kheradvar, A.; Gharib, M. On Mitral Valve Dynamics and its Connection to Early Diastolic Flow. *Ann. Biomed. Eng.* **2008**, *37*, 1–13. [CrossRef]
13. Espa, S.; Badas, M.G.; Fortini, S.; Querzoli, G.; Cenedese, A. A Lagrangian investigation of the flow inside the left ventricle. *Eur. J. Mech. B Fluids* **2012**, *35*, 9–19. [CrossRef]
14. Reul, H.; Talukder, N.; Mu¨ller, E. Fluid mechanics of the natural mitral valve. *J. Biomech.* **1981**, *14*, 361–372. [CrossRef]
15. Voorneveld, J.; Saaid, H.; Schinkel, C.; Radeljic, N.; Lippe, B.; Gijsen, F.J.; van der Steen, A.F.; de Jong, N.; Claessens, T.; Vos, H.J.; et al. 4-D Echo-Particle Image Velocimetry in a Left Ventricular Phantom. *Ultrasound Med. Biol.* **2020**, *46*, 805–817. [CrossRef]
16. Warner, H.R.; Toronto, A.F. Effect of Heart Rate on Aortic Insufficiency as Measured by a Dye-Dilution Technique. *Circ. Res.* **1961**, *9*, 413–417. [CrossRef]
17. Raffel, M.; Willert, C.E.; Scarano, F.; Kähler, C.J.; Wereley, S.T.; Kompenhans, J. *Particle Image Velocimetry: A Practical Guide*, 3rd ed.; Springer International Publishing: Cham, Switzerland, 2018.
18. Scharnowski, S.; Kähler, C.J. Particle image velocimetry—Classical operating rules from today's perspective. *Opt. Lasers Eng.* **2020**, *135*, 106185. [CrossRef]
19. Faludi, R.; Szulik, M.; D'Hooge, J.; Herijgers, P.; Rademakers, F.; Pedrizzetti, G.; Voigt, J.-U. Left ventricular flow patterns in healthy subjects and patients with prosthetic mitral valves: An in vivo study using echocardiographic particle image velocimetry. *J. Thorac. Cardiovasc. Surg.* **2010**, *139*, 1501–1510. [CrossRef]
20. Akiyama, K.; Maeda, S.; Matsuyama, T.; Kainuma, A.; Ishii, M.; Naito, Y.; Kinoshita, M.; Hamaoka, S.; Kato, H.; Nakajima, Y.; et al. Vector flow mapping analysis of left ventricular energetic performance in healthy adult volunteers. *BMC Cardiovasc. Disord.* **2017**, *17*, 21. [CrossRef]
21. Watanabe, H.; Sugiura, S.; Hisada, T. The looped heart does not save energy by maintaining the momentum of blood flowing in the ventricle. *Am. J. Physiol. Circ. Physiol.* **2008**, *294*, H2191–H2196. [CrossRef] [PubMed]
22. Seo, J.H.; Mittal, R. Effect of diastolic flow patterns on the function of the left ventricle. *Phys. Fluids* **2013**, *25*, 110801. [CrossRef]
23. Suh, G.-Y.; Les, A.S.; Tenforde, A.S.; Shadden, S.C.; Spilker, R.L.; Yeung, J.J.; Cheng, C.P.; Herfkens, R.J.; Dalman, R.L.; Taylor, C.A. Quantification of Particle Residence Time in Abdominal Aortic Aneurysms Using Magnetic Resonance Imaging and Computational Fluid Dynamics. *Ann. Biomed. Eng.* **2010**, *39*, 864–883. [CrossRef]
24. De Vecchi, A.; Marlevi, D.; Nordsletten, D.A.; Ntalas, I.; Leipsic, J.; Bapat, V.; Rajani, R.; Niederer, S.A. Left ventricular outflow obstruction predicts increase in systolic pressure gradients and blood residence time after transcatheter mitral valve replacement. *Sci. Rep.* **2018**, *8*, 1–11. [CrossRef] [PubMed]
25. Reza, M.M.S.; Arzani, A. A critical comparison of different residence time measures in aneurysms. *J. Biomech.* **2019**, *88*, 122–129. [CrossRef]
26. Bolger, A.F.; Heiberg, E.; Karlsson, M.; Wigström, L.; Engvall, J.; Sigfridsson, A.; Ebbers, T.; Kvitting, J.-P.; Carlhäll, C.J.; Wranne, B. Transit of Blood Flow Through the Human Left Ventricle Mapped by Cardiovascular Magnetic Resonance. *J. Cardiovasc. Magn. Reson.* **2007**, *9*, 741–747. [CrossRef]
27. Hendabadi, S.; Bermejo, J.; Benito, Y.; Yotti, R.; Fernández-Avilés, F.; Del Alamo, J.C.; Shadden, S.C. Topology of blood transport in the human left ventricle by novel processing of Doppler echocardiography. *Ann. Biomed. Eng.* **2013**, *41*, 2603–2616. [CrossRef] [PubMed]
28. Rossini, L.; Martinez-Legazpi, P.; Vu, V.; Friera, L.F.; del Villar, C.P.; Rodríguez-López, S.; Benito, Y.; Borja, M.-G.; Pastor-Escuredo, D.; Yotti, R.; et al. A clinical method for mapping and quantifying blood stasis in the left ventricle. *J. Biomech.* **2015**, *49*, 2152–2161. [CrossRef]
29. Goode, D.; Dhaliwal, R.; Mohammadi, H. Transcatheter Mitral Valve Replacement: State of the Art. *Cardiovasc. Eng. Technol.* **2020**, *11*, 229–253. [CrossRef]
30. Domenichini, F.; Pedrizzetti, G.; Baccani, B. Three-dimensional filling flow into a model left ventricle. *J. Fluid Mech.* **2005**, *539*, 179–198. [CrossRef]